NATIONAL ADVISORY COMMITTEE FOR AERONAUTICS

TECHNICAL NOTE

No. 1267

FLIGHT TESTS OF A HELICOPTER IN AUTOROTATION,

INCLUDING A COMPARISON WITH THEORY
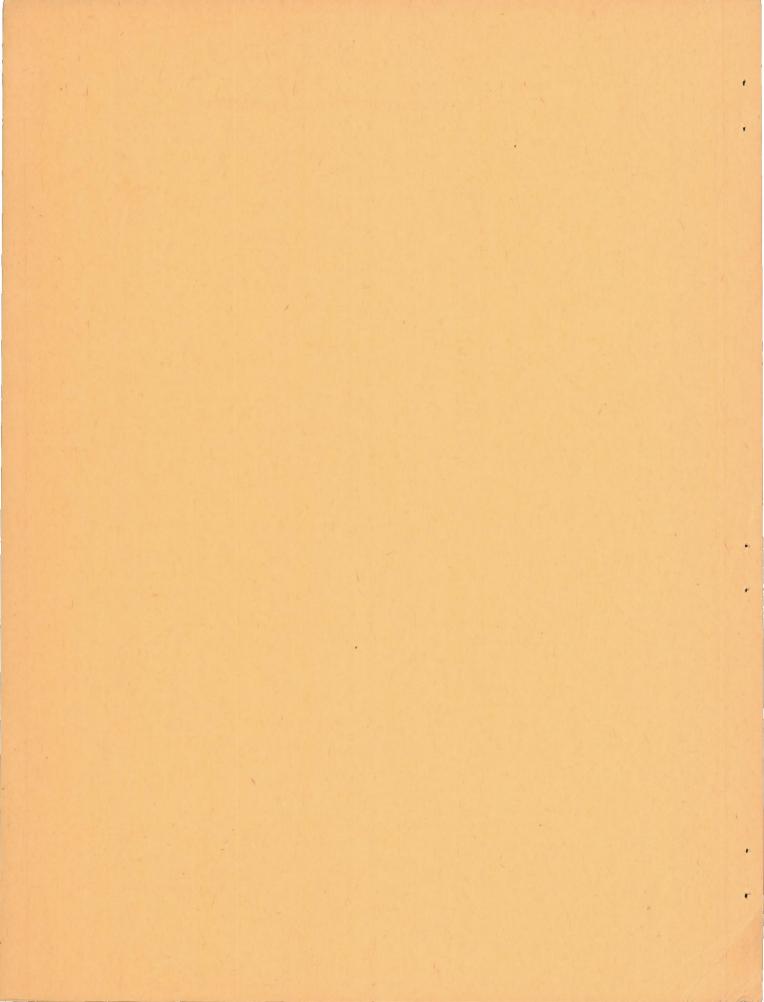
By Alfred Gessow and Garry C. Myers, Jr.

Langley Memorial Aeronautical Laboratory
Langley Field, Va.

Washington

April 1947

NATIONAL ADVISORY COMMITTEE FOR AERONAUTICS

———

TECHNICAL NOTE NO. 1267

———

FLIGHT TESTS OF A HELICOPTER IN AUTOROTATION,

INCLUDING A COMPARISON WITH THEORY

By Alfred Gessow and Garry C. Myers, Jr.

SUMMARY

The results of glide performance tests conducted on a test helicopter with its original production blades in the autorotation condition are presented. The data were reduced to coefficient form, and performance at standard sea-level conditions was calculated. The experimentally determined rotor drag-lift ratios were compared with theoretical calculations, and a similar comparison was made for previously obtained power-on flight data. In addition, the improvement in power-off (autorotation) performance that results from operating with aerodynamically cleaner blades was investigated.

The helicopter was found to have a minimum rate of descent at sea level of 1080 feet per minute at an airspeed of approximately 40 miles per hour. The maximum lift-drag ratio of the helicopter was 3.9, and the highest lift-drag ratio obtained for the main rotor was 6.7. Good agreement between theory and experiment was obtained when theoretical calculations were based on a profile-drag polar that corresponded to "rough" airfoil sections. Inasmuch as similar agreement was obtained between theoretical and experimental data in power-on level flight, the theory is considered useful in extending the available rotor data from one condition to the other. It was found that the use of aerodynamically cleaner blades resulted in significant gains in gliding performance. For the helicopter tested it appeared that a 22-percent reduction in profile-drag coefficient would result in a $6\frac{1}{2}$-percent reduction in the minimum rate of descent.

INTRODUCTION

Flight tests are being conducted by the Flight Research Division of the Langley Laboratory on a conventional single-rotor helicopter as part of a general program of helicopter research. These tests

include performance measurements in level flight, hovering, glides, and climbs, and camera observations of blade motion in selected conditions. This paper presents the results of power-off (autorotation) performance measurements that were made with the original production set of main-rotor blades.

In the event of power failure the helicopter rotor becomes, in effect, an autogiro rotor. Safety and design considerations make this autorotative condition important to the helicopter designer. Data obtained with the test helicopter in autorotation were taken in order to provide information which could be used in improving the autorotative characteristics of helicopters. The tests also provided an opportunity to compare the same rotor in the power-on and autorotative conditions, without the introduction of uncertainties due to differences in blade parameters which are present when two different rotors are tested and compared in the two conditions. The glide data thus permitted a check of the theoretically predicted rotor drag-lift ratios in both power-on and power-off flight. Once the relationship between the two conditions is established, the available information on the autogiro and the helicopter becomes interrelated.

SYMBOLS

W gross weight of helicopter, pounds

V_c calibrated airspeed (indicated airspeed corrected for instrument and installation errors; can be considered

equal to $V\sqrt{\rho/\rho_0}$ in the present case), miles per hour

V true airspeed, miles per hour

V_h horizontal component of true airspeed, miles per hour

V_v rate of descent; vertical component of true airspeed, feet per minute

R rotor-blade radius, feet

Ω rotor angular velocity, radians per second

ρ mass density of air, slugs per cubic foot

ρ_0 mass density of air at sea level under standard conditions (0.002378 slug per cubic foot)

μ tip-speed ratio $\left(\dfrac{V \cos \alpha}{\Omega R}\right)$

α rotor angle of attack; angle between projection in plane of symmetry of axis about which there is no cyclic pitch change and a line perpendicular to flight path, positive when axis is pointing rearward, degrees

α_f fuselage angle of attack; angle between relative wind and a line in plane of symmetry and perpendicular to main-rotor-shaft axis, positive when nose is up, degrees

$\Delta\alpha_f$ correction to fuselage angle of attack to allow for rotor downwash, degrees (assumed equal to $-57.3C_L/4$)

α_{f_c} corrected fuselage angle of attack, degrees $(\alpha_f + \Delta\alpha_f)$

C_{L_f} fuselage lift coefficient $\left(\dfrac{\text{Fuselage lift}}{\frac{1}{2}\rho V^2 \pi R^2}\right)$

C_{D_f} fuselage drag coefficient $\left(\dfrac{\text{Fuselage drag}}{\frac{1}{2}\rho V^2 \pi R^2}\right)$

γ glide-path angle; that is, angle of which tangent is rate of descent divided by horizontal component of velocity, degrees

$C_{L_{uncor}}$ uncorrected rotor lift coefficient $\left(\dfrac{W \cos \gamma}{\frac{1}{2}\rho V^2 \pi R^2}\right)$

C_L rotor lift coefficient $\left(C_{L_{uncor}} - C_{L_f}\right)$

L rotor lift, pounds $(W \cos \gamma - \text{fuselage lift})$

T rotor thrust, pounds $\left(\dfrac{L}{\cos \alpha}\right)$

C_T thrust coefficient $\left(\dfrac{T}{\pi R^2 \rho (\Omega R)^2}\right)$

$\left(\dfrac{D}{L}\right)_g$ over-all drag-lift ratio of helicopter $(\tan \gamma)$

$\left(\dfrac{D}{L}\right)_p$ parasite drag of fuselage, rotor head, and blade shanks, divided by main-rotor lift

$\dfrac{P}{L}$ shaft power parameter (The symbol P is equal to the rotor-shaft power divided by the velocity along the flight path; in autorotation, P/L is negative and represents the power supplied by the rotor to overcome the gearing and bearing frictional losses and to drive the tail rotor)

$\left(\dfrac{D}{L}\right)_i$ induced drag-lift ratio (taken herein as $C_L/4$)

$\left(\dfrac{D}{L}\right)_o$ rotor profile drag-lift ratio

$\left(\dfrac{D}{L}\right)_r$ drag-lift ratio of main rotor; that is, ratio of equivalent drag of main rotor to rotor lift

$$\left(\left(\dfrac{D}{L}\right)_i + \left(\dfrac{D}{L}\right)_o\right)$$

σ solidity $\left(\dfrac{bc_e}{\pi R}\right)$ (for the present case, $\sigma = 0.060$)

c_e equivalent chord $\left(\dfrac{\displaystyle\int_0^R cr^2\,dr}{\displaystyle\int_0^R r^2\,dr}\right)$

c local chord

r radius to blade element

a slope of curve of lift coefficient against section angle of attack (radian measure; assumed equal to 5.73)

c_{d_o} blade section profile-drag coefficient

α_o blade section angle of attack, measured from zero lift, radians

θ_m average main rotor-blade pitch, uncorrected for play in linkage or for mean blade twist, degrees

APPARATUS AND TEST PROCEDURE

The tests were conducted with a Sikorsky HNS-1 (YR-4B) helicopter, the dimensions and pertinent characteristics of which are shown in figure 1. Other particulars, including a detailed description of the fabric-covered original main-rotor blades, are given in references 1 and 2.

Quantities measured during the power-off glide tests included the following:

Airspeed	Free-air static pressure
Rotor speed	Main-rotor pitch
Main-rotor-shaft torque	Tail-rotor pitch
Tail-rotor-shaft torque	Attitude angle (shaft inclination)
Free-air temperature	Cyclic-pitch control position

The methods by which these quantities were obtained are discussed in reference 1.

In gliding flight the quantities which most critically affect the accuracy of the results are airspeed and rate of descent, and they are therefore considered worthy of special discussion.

Airspeed was determined by means of a freely swiveling pitot-static installation mounted on the end of a long boom in front of the fuselage, the airspeed head being about two feet in front of the main rotor disk (fig. 2). The installation was calibrated by means of a trailing pitot-static "bomb" suspended approximately 100 feet below the rotor. The calibration data obtained are shown in figure 3.

Atmospheric pressure measurements that were necessary for calculation of rates of descent were continuously recorded throughout each run.

Flight procedure consisted in making glides from about 5,000 feet to 3,000 feet pressure altitude, the airspeed and pitch setting being held constant. Variations in thrust coefficient were achieved by operating at different pitch settings and therefore at different rotational speeds.

REDUCTION OF DATA

Rotor drag-lift ratios $(D/L)_r$ were calculated from the general performance equation expressed in coefficient form as

$$\frac{P}{L} = \left(\frac{D}{L}\right)_r + \left(\frac{D}{L}\right)_p - \left(\frac{D}{L}\right)_g$$

For each test point, values of $(D/L)_g$, P/L, and $(D/L)_p$ were determined from measurements taken. Values of $(D/L)_g$, which represent the tangent of the angle of glide, were calculated from the airspeed and rate of descent. These rates of descent were calculated by means of plots of static pressure against time together with a mean free-air temperature value for the descent. With the rotor in autorotation, P/L is a small negative quantity that represents the power supplied by the rotor to overcome the gearing and bearing frictional losses and to drive the tail rotor. This quantity P/L was determined from recorded shaft torque and rotor rotational speed. Values of $(D/L)_p$ were calculated with the aid of full-scale wind-tunnel tests on the fuselage and hub of the test helicopter (fig. 4). The main-rotor drag-lift ratio was then calculated as

$$\left(\frac{D}{L}\right)_r = \left(\frac{D}{L}\right)_g - \left(\frac{D}{L}\right)_p + \frac{P}{L}$$

The method of reducing the data to coefficient form parallels that of reference 1. Certain of the assumptions used in the level-flight analysis were modified, however, to comply with gliding-flight conditions and are as follows:

(1) Rotor lift is calculated by multiplying the helicopter gross weight by the cosine of the glide angle and subtracting the fuselage lift. Rotor thrust, which was considered equal to rotor lift in level flight, was assumed equal to rotor lift divided by the cosine of the rotor angle of attack α, the value of α being determined as in reference 1.

(2) The drag force on the tail rotor was found (by the method used in reference 1) to amount to less than 1 percent of the fuselage drag in the autorotation condition and was consequently neglected.

RESULTS AND DISCUSSION

The test data are presented in table I. Drag-lift ratios and other parameters derived from the data are given in table II.

Helicopter glide performance.- In order to obtain the variation of helicopter rate of descent with airspeed, unaffected by variations of weight and density, the experimental data were first plotted in the coefficient form shown in figure 5. The abscissa, $1/\sqrt{C_L}$ is a velocity parameter which is directly proportional to the true

velocity and which effectively resolves variations of weight and density into equivalent velocity changes. The data are grouped according to thrust coefficients but, because of the limited data available and the scatter in the data which covered any trend with C_T, a single curve was drawn to represent an average thrust coefficient of 0.0052 (average weight 2520 lb, $\frac{\rho}{\rho_0} = 0.92$). The data indicate a minimum value of $(D/L)_g$ of 0.26 in the range of $1/\sqrt{C_L}$ between 2.0 to 2.2 corresponding to a maximum value of lift-drag ratio of 3.9 at approximately 65 miles per hour.

The nondimensional data of figure 5 can be expressed in terms of rate of descent and velocity for any desired combination of weight and air density. In figure 6, the faired experimental curve of figure 5 has been reduced to standard conditions, that is, normal gross weight of 2520 pounds and sea-level density.

At sea-level conditions and normal weight, figure 6 shows that the test helicopter has a minimum rate of descent of 1080 feet per minute at about 40 miles per hour. This speed corresponds to the speed range between 40 and 45 miles per hour for minimum power in level flight. (See fig. 8 of reference 1.) The minimum angle of glide can be found from figure 6 to be approximately 14° and to occur at a rate of descent of 1400 feet per minute and at an airspeed of approximately 64 miles per hour.

In obtaining the present flight data, emphasis was placed upon the determination of the glide characteristics over the higher speed range, that is, minimum rate of descent and minimum angle of glide. A few measurements were also made in vertical descent. As a result of the difficulty in holding zero horizontal speed, however, the maximum rate of descent obtained, 2140 feet per minute when reduced to sea-level conditions, may have been as much as 10 percent too low because of the presence of some horizontal velocity during the measurements. The effect of small horizontal velocities on the rate of descent in autorotation can be estimated from figure 7, which presents glide data obtained with the PCA-2 autogiro (reference 3). The figure indicates that horizontal airspeeds between 5 and 10 miles per hour can effect a reduction in the rate of descent of the order of 10 percent.

Rotor drag-lift ratios.- In order to study the efficiency of the rotor itself, the D/L equivalent of the fuselage and residual shaft power losses have been subtracted from the over-all drag-lift ratio $(D/L)_g$, as described in the section "Reduction of Data." The resulting rotor drag-lift ratios are plotted in figure 8 against the velocity parameter $1/\sqrt{C_L}$. The lowest average value of measured main-rotor D/L shown in the figure is about 0.15, corresponding

to an L/D of 6.7. Inasmuch as the trend of the data does not appear to indicate that a minimum has been reached, higher L/D's might be expected at higher speeds.

Comparison of rotor drag-lift ratio with theory.- Theoretically predicted values of $(D/L)_r$ are compared with flight data in figure 8. Inasmuch as the experimental data showed no trend for the variation of $(D/L)_r$ with C_T (because of the small range of C_T's covered in the tests, the limited data taken, and the scatter among them), theoretical $(D/L)_r$ curves representing an average C_T of 0.0052 were drawn.

The theoretical curves were calculated from the performance charts of reference 4, which were extended to include tip-speed ratios equal to 0.10. These charts are based on a blade-section profile-drag polar represented by the equation

$$c_{d_o} = 0.0087 - 0.0216\ \alpha_o + 0.400\ \alpha_o^2$$

This variation of drag coefficient with section angle of attack is representative of conventional, semismooth airfoils (smooth airfoils increased by a roughness factor of 17 percent). Theory based on such a drag polar may properly be called "semismooth blade" theory and the curve is labeled as such in figure 8. In order, however, to take into account the imperfect profile and deformable surfaces of the fabric-covered blades tested (see reference 2), the theory was also calculated by increasing the rotor profile drag-lift ratios obtained from the performance charts by 28 percent, thus allowing a total roughness factor of 50 percent. The "rough-blade" theoretical curve in figure 8 was calculated in this manner.

Good agreement between the average experimental rotor drag-lift ratios and the rough-blade theoretical values is indicated by figure 8. The difference between the two theoretical curves in the figure shows that the lift and drag characteristics of the rotor-blade sections must be known in order to predict the rotor performance with sufficient accuracy.

It is interesting to determine whether the same theory that was used for the autorotational condition could be used to predict the performance of rotors in the power-on condition. Level-flight data, obtained with the same set of blades used in the autorotation tests, afford an excellent opportunity to check the theory in the two flight conditions. From this data, the influence of secondary effects due to differences in blade construction and solidity which, for example, might be present if two different rotors were tested,

is eliminated. Experimental drag-lift ratios, obtained at an average $C_T = 0.0054$ and taken from reference 1, are compared with results obtained by the rough-blade theory in figure 9. The figure indicates good agreement between theory and experiment for level flight, as was true in the autorotative case shown in figure 8.

In addition to presenting a comparison between theory and experiment, figures 8 and 9 show that the theoretical calculations predict rotor performance in the two conditions with sufficient accuracy to make the theory useful in extending the scope of helicopter and autogiro rotor data to either operating state.

Performance gains to be expected with smoother blades.- Rotor drag-lift ratios obtained from full-scale-tunnel tests on a rotor with relatively smooth plywood-covered blades are compared in figure 10 with values calculated for semismooth blades. The agreement shown suggests that if smooth, rigid-surfaced blades were used on the test helicopter, the resulting performance would be in similar agreement with the curve based on use of semismooth blade theory shown in figure 8. The improvement in the glide performance of the helicopter equipped with rotor blades aerodynamically cleaner than the original blades is shown in figure 11. The curve in figure 11 labeled "original blades" corresponds to the measured performance and was taken from figure 6, whereas the curve adjusted for semismooth blades was calculated by reducing the measured rate of descent by an amount equivalent to the difference (shown in fig. 8) between the theoretical values of $(D/L)_r$ for the rough and the semismooth blades. Thus, the minimum rate of descent would be reduced from 1080 to 1010 feet per minute and the minimum glide angle would be reduced by 9 percent if cleaner blades were used.

In order to evaluate properly the improvement in glide performance effected by a reduction in rotor profile drag, the contribution of the parasite and induced drag losses are also shown in figure 11. It can be seen that a helicopter with a light disk loading and a cleaner fuselage would benefit more, on a percentage basis, from an increase in blade cleanness than the helicopter under test. For example, the 22-percent reduction in the rotor profile drag due to changing to semismooth blades would result in a reduction of 70 feet per minute or $6\frac{1}{2}$ percent in the minimum rate of descent of the helicopter tested. If the rates of descent due to the parasite and induced drag were removed, however, the minimum rate of descent would become 500 feet per minute. In this case the 70 feet per minute would represent 14 percent of the minimum rate of descent. A 22-percent reduction in rotor profile drag may thus decrease the minimum rate of descent as much as 14 percent, depending on the amount of induced and parasite losses present.

CONCLUSIONS

From the data obtained with a conventional single-rotor heli-copter as tested in autorotation and the accompanying theoretical analysis, the following conclusions are indicated:

1. For operation at sea level, a minimum rate of descent of 1080 feet per minute was obtained at an airspeed of about 40 miles per hour.

2. The maximum lift-drag ratio of the helicopter as tested was 3.9. The highest lift-drag ratio obtained for the main rotor over the available speed range was 6.7.

3. Good agreement between theoretical and experimental auto-rotation performance was obtained when theoretical calculations were based on a profile-drag polar corresponding to "rough" airfoil sections.

4. The same theory can satisfactorily predict the performance of a rotor in both the power-off and power-on flight conditions.

5. Since theory can satisfactorily predict rotor performance in both the autorotation and power-on conditions, it is considered useful in extending the available rotor data from one condition to the other.

6. Significant improvement in gliding performance appears possible with improved blade contour and surface condition. For the helicopter tested, a reduction of 22 percent in profile-drag coefficient (obtained by operating with "semismooth" instead of "rough" blades) would result in a $6\frac{1}{2}$-percent reduction in the minimum rate of descent.

Langley Memorial Aeronautical Laboratory
    National Advisory Committee for Aeronautics
        Langley Field, Va., February 17, 1947

REFERENCES

1. Gustafson, F. B.: Flight Tests of the Sikorsky HNS-1 (Army YR-4B)
     Helicopter. I - Experimental Data on Level-Flight Performance
     with Original Rotor Blades. NACA MR No. L5C10, 1945.

2. Gustafson, F. B., and Gessow, Alfred: Flight Tests of the Sikorsky
     HNS-1 (Army YR-4B) Helicopter. II - Hovering and Vertical-
     Flight Performance with the Original and an Alternate Set
     of Main-Rotor Blades, Including a Comparison with Hovering
     Performance Theory. NACA MR No. L5D09a, 1945.

3. Wheatley, John B.: Lift and Drag Characteristics and Gliding
     Performance of an Autogiro as Determined in Flight.
     NACA Rep. No. 434, 1932.

4. Bailey, F. J., Jr., and Gustafson, F. B.: Charts for Estimation
     of the Characteristics of a Helicopter Rotor in Forward Flight.
     I - Profile Drag-Lift Ratio for Untwisted Rectangular Blades.
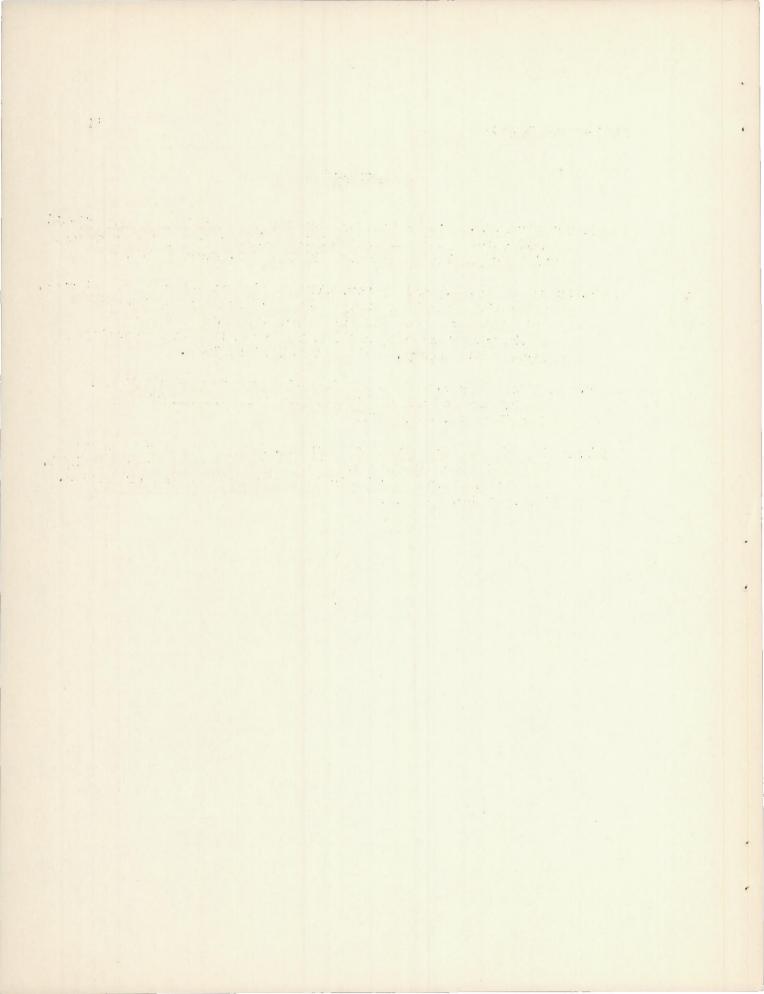   NACA ACR No. L4H07, 1944.

TABLE I

SUMMARY OF FLIGHT DATA IN AUTOROTATION

Test run	Calibrated airspeed V_c (mph)	Density ratio, ρ/ρ_0 (av.)	True airspeed, V (mph)	Gross weight, W (lb)	Rotor speed (rpm)	Rate of descent V_v (fpm)	Atmospheric pressure (in. Hg) (av.)	Free-air temperature (°F)	Main rotor power (hp)	Tail rotor power (hp)	Pitch angle (deg) Main rotor	Pitch angle (deg) Tail rotor	Shaft inclination (nose down) (deg)	Center of gravity position, ahead of shaft (in.)	Stick position, forward (in.) (a)	Stick position, left (in.) (a)	Yaw angle (deg)
1	46.1	0.943	47.5	2546	230	1080	28.78	70	-5.4	3.7	2.5	-0.8	2.1	0.6	2.5	1.4	9.3
2	54.1	.944	55.7	2578	224	1176	28.98	73	-3.2	3.6	3.0	-3.1	3.1	1.2	--------	1.5	6.9
3	48.1	.945	49.5	2569	218	1260	28.99	73	-4.4	3.5	3.1	-3.4	3.3	1.3	--------	1.6	10.6
4	51.0	.941	52.6	2561	225	1250	28.91	73	-4.6	3.4	2.8	-2.9	3.4	1.4	--------	1.4	2.4
5	47.0	.969	47.7	2498	214	1035	27.38	30	-5.2	3.7	3.1	-1.4	1.9	2.0	1.8	1.1	0.9
6	42.4	.931	43.9	2533	223	1080	28.27	67	-4.4	3.0	3.5	-1.3	0.9	0.8	2.5	1.3	0.7
7	53.1	.929	55.1	2527	225	1240	28.33	70	-5.0	4.1	3.7	-1.6	2.4	0.9	3.2	1.5	0.7
8	64.1	.938	66.2	2515	225	1540	28.74	72	-6.0	3.1	3.5	-1.9	4.1	1.0	3.5	1.5	1.5
9	53.6	.924	55.8	2503	208	1190	28.30	72	-4.6	2.9	4.4	-1.8	3.1	1.1	3.3	1.6	0
10	55.3	.927	57.4	2491	232	1275	28.38	71	-5.1	4.0	2.9	-1.7	3.0	1.3	2.6	1.0	-0.2
11	66.7	.935	69.0	2485	226	1600	28.54	71	-5.0	4.1	3.5	-1.9	4.8	1.4	3.1	1.2	0.6
12	54.6	.939	56.4	2479	197	1306	28.77	72	-4.3	2.9	4.8	-1.7	3.1	1.4	3.3	1.6	0.3
13	38.2	.787	43.1	2478	218	1290	22.62	38	-5.3	2.9	4.0	-1.6	2.0	1.4	2.0	1.5	-3.7
14	40.2	.871	43.1	2478	210	1184	25.25	45	-5.2	2.9	4.0	-1.6	2.0	1.4	2.0	1.5	-1.6
15	43.6	.948	44.8	2478	225	1170	28.00	52	-5.6	2.9	2.9	-1.5	2.3	1.4	1.9	1.0	-2.5
16	65.0	.883	69.2	2523	220	1520	27.10	73	-----	----	3.6	-2.9	4.3	0.5	3.8	1.9	-3.7
17	64.9	.892	68.7	2505	220	1450	27.40	73	-----	----	3.7	-3.0	4.5	0.7	3.5	1.7	-3.4
18	69.0	.923	71.8	2571	222	1620	28.69	80	-----	----	-----	-----	5.5	1.2	4.1	1.9	1.8
19	64.7	.906	68.0	2571	225	1470	28.20	80	-----	----	-----	-----	4.9	1.2	3.6	1.8	4.1
20	73.7	.913	77.1	2559	226	1650	28.42	80	-5.7	----	4.3	-1.7	6.2	1.3	3.5	1.9	2.9

[a]Cyclic pitch variation, in degrees from mean value is 1.25 × stick position.

NATIONAL ADVISORY
COMMITTEE FOR AERONAUTICS

TABLE II
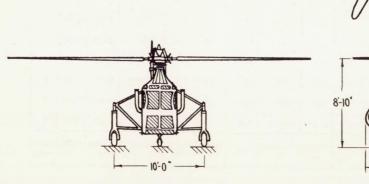
ROTOR DRAG-LIFT RATIOS AND RELATED PARAMETERS

DERIVED FROM AUTOROTATION FLIGHT DATA

Test run	V_c (mph)	V (mph)	V_v (ft/min)	θ_m (deg)	α (deg)	μ	c_L (uncor.)	$\Delta\alpha_f$ (deg)	α_{f_c} (deg)	Δc_L	c_L	$\dfrac{c_L}{\sigma}$	c_T	$\dfrac{2c_T}{\sigma a}$	P/L	$(D/L)_g$	$(D/L)_p$	$(D/L)_r$	γ (deg)
1	46.1	47.5	1080	2.5	10	0.150	0.399	-5.7	7.2	-0.001	0.398	6.63	0.0047	0.0273	-0.015	0.268	0.045	0.208	15.0
2	54.1	55.7	1176	3.0	8	.182	.295	-4.2	6.6	-.001	.294	4.90	.0050	.0290	-.012	.248	.060	.176	13.9
3	48.1	49.5	1260	3.1	11	.164	.366	-5.2	8.3	-.001	.365	6.08	.0052	.0302	-.013	.302	.049	.240	16.8
4	51.0	52.6	1250	2.8	10	.170	.327	-4.7	7.6	-.002	.325	5.42	.0049	.0285	-.013	.281	.054	.214	15.7
5	47.0	47.7	1035	3.1	10	.162	.379	-5.4	7.0	-.001	.378	6.30	.0052	.0302	-.013	.255	.047	.195	14.3
6	42.4	43.9	1080	3.5	12	.142	.468	-6.7	8.6	-.002	.466	7.77	.0050	.0290	-.015	.291	.039	.237	16.2
7	53.1	55.1	1240	3.7	9	.179	.299	-4.3	8.1	-.001	.298	4.97	.0049	.0285	-.013	.264	.061	.190	14.8
8	64.1	66.2	1540	3.5	7	.215	.204	-2.9	8.3	-.002	.202	3.37	.0048	.0279	-.011	.274	.090	.173	15.3
9	53.6	55.8	1190	4.4	7	.196	.291	-4.2	6.7	-.001	.290	4.83	.0057	.0331	-.010	.249	.062	.177	14.0
10	55.3	57.4	1275	2.9	9	.180	.272	-3.9	7.7	-.001	.271	4.52	.0046	.0267	-.013	.261	.067	.181	14.6
11	66.7	69.0	1600	3.5	7	.223	.186	-2.6	7.8	-.001	.185	3.08	.0048	.0279	-.011	.274	.098	.165	15.3
12	54.6	56.4	1306	4.8	8	.208	.276	-4.0	8.2	-.001	.275	4.58	.0062	.0360	-.009	.274	.066	.199	15.3
13	38.2	43.1	1290	4.0	16	.140	.550	-7.9	10.0	-.003	.547	9.12	.0060	.0349	-.016	.362	.033	.313	19.9
14	40.2	43.1	1184	4.0	14	.148	.502	-7.2	9.0	-.002	.500	8.34	.0059	.0343	-.014	.329	.036	.279	18.2
15	43.6	44.8	1170	2.9	13	.143	.429	-6.1	8.9	-.002	.427	7.12	.0047	.0273	-.016	.312	.042	.254	17.3
16	65.0	69.2	1520	3.6	6	.231	.199	-2.9	7.3	-.001	.198	3.30	.0053	.0308	-.010	.259	.089	.160	14.5
17	64.9	68.7	1450	3.7	5	.229	.199	-2.9	6.5	0	.199	3.32	.0052	.0302	-.010	.248	.089	.149	13.9
18	69.0	71.8	1620	-----	5	.238	.180	-2.6	6.8	-.001	.179	2.98	.0051	.0296	-.009	.266	.106	.151	14.9
19	64.7	68.0	1470	-----	5	.222	.205	-2.9	6.4	0	.205	3.42	.0051	.0296	-.010	.253	.092	.151	14.2
20	73.7	77.1	1650	4.3	4	.252	.158	-2.3	4.8	0	.158	2.63	.0050	.0290	-.008	.249	.120	.121	14.0

NATIONAL ADVISORY
COMMITTEE FOR AERONAUTICS

Gross weight (as flown), lb 2520
Disk loading, lb/sq ft 2.22
Tip speed (normal)
   Main rotor, fps 447
   Tail rotor, fps 494
Rotor solidity 0.06
Distance from center line of main rotor
   to center line of tail rotor, ft 25.2
Parasite drag area, sq ft 23

NATIONAL ADVISORY
COMMITTEE FOR AERONAUTICS

Figure 1.- Dimensions and characteristics of test helicopter.

Fig. 1
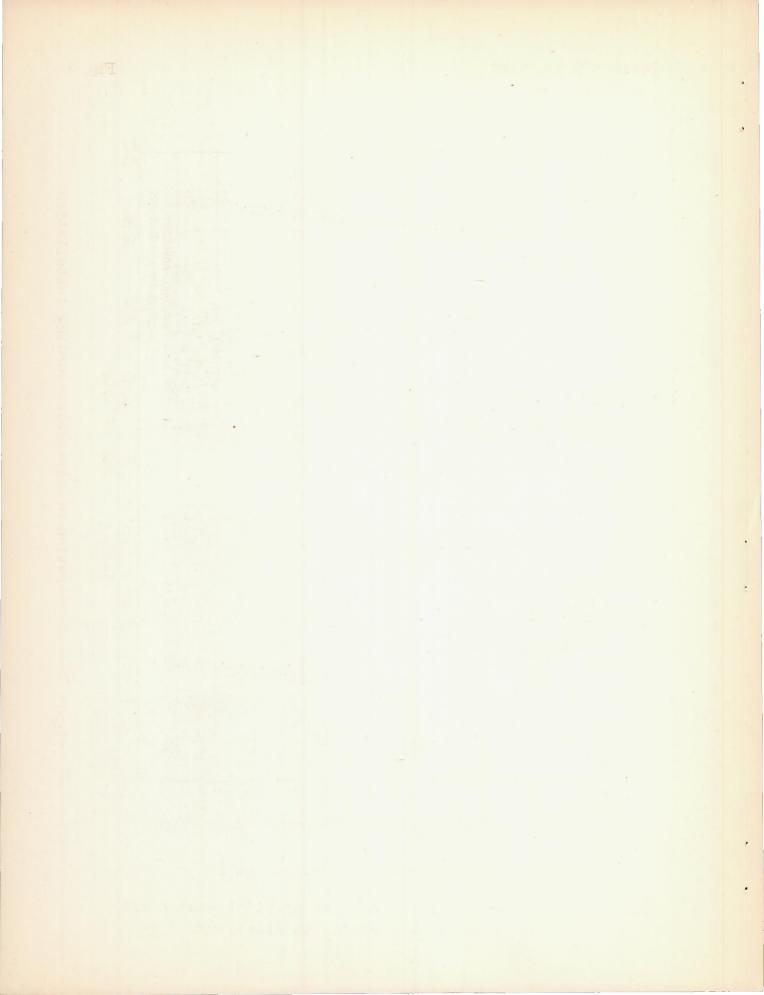
(a) General view.

(b) Close-up view of airspeed head.

Figure 2.- Airspeed boom and details of pitot-static and
flow-angle pressure-tube installations.

Fig. 3
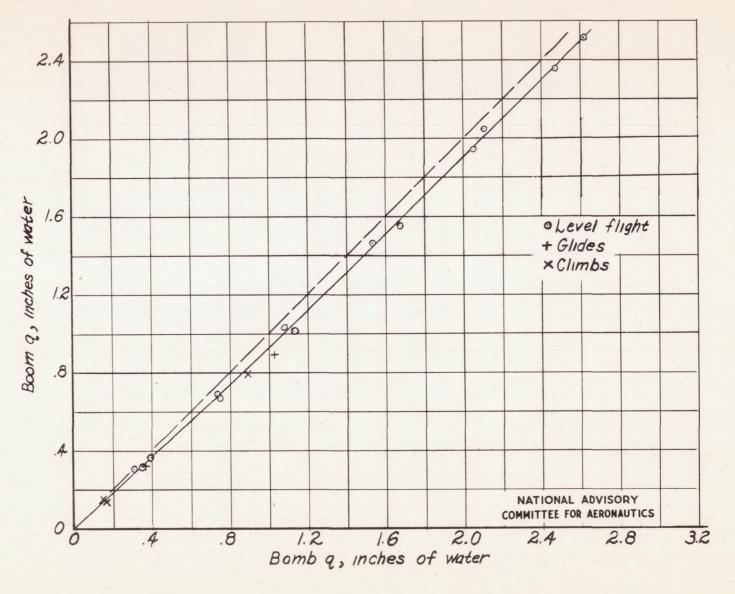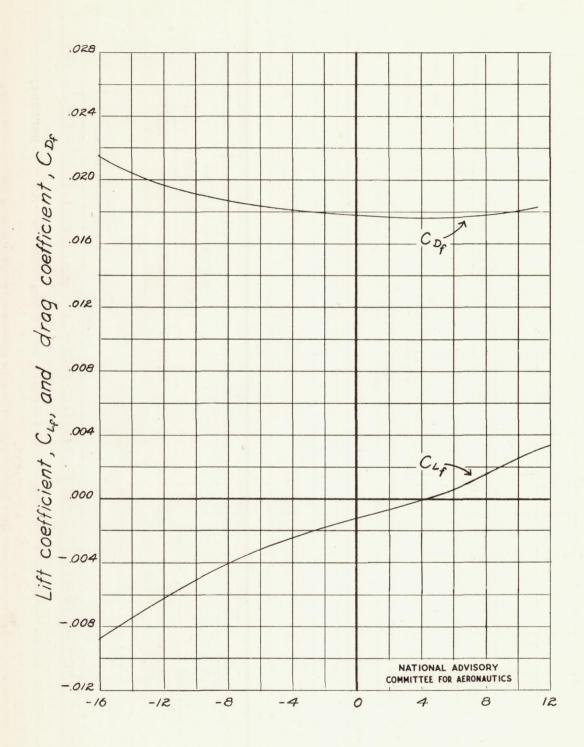
Figure 3.-   Calibration of airspeed-recording installation.

Fig. 4   NACA TN No. 1267

Figure 4.- Fuselage drag and lift coefficients (based on rotor-disk area) obtained in Langley full-scale tunnel and used in reduction of data for test helicopter.

Fig. 5

Figure 5.– Drag–lift ratio $\left(\dfrac{D}{L}\right)_g$ against velocity parameter $\dfrac{1}{\sqrt{C_L}}$ for test helicopter in autorotative flight. Gross weight as flown, 2520 pounds ± 2 percent; density ratio $\dfrac{\rho}{\rho_0}$, 0.92 ± 4 percent.
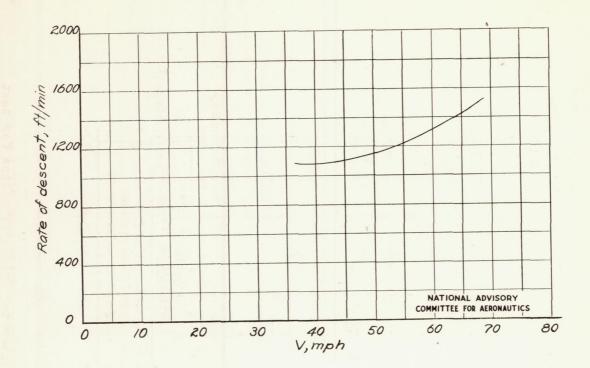
Figure 6.- Autorotative performance of test helicopter reduced to standard sea-level conditions, derived from faired curve of figure 4. Gross weight, 2520 pounds.
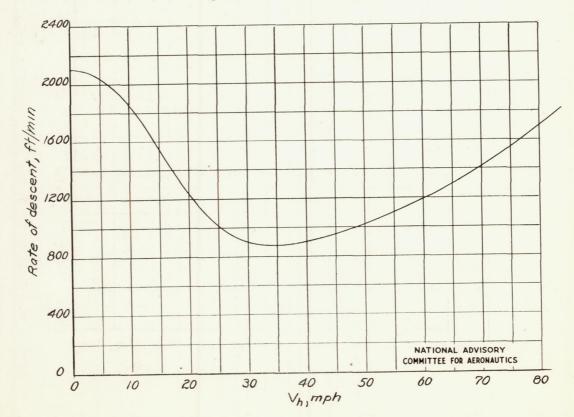
Figure 7.- Effect of horizontal velocity on autorotative rates of descent (from reference 3).
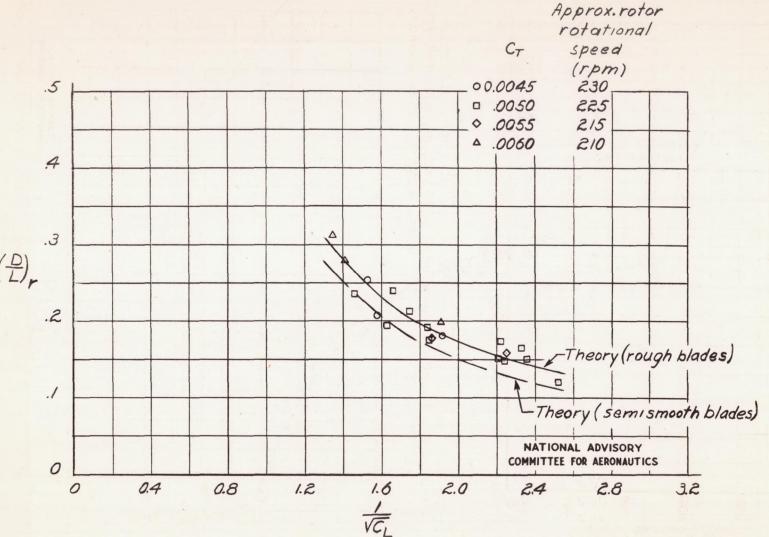
Figure 8.- Comparison of experimental and theoretical main-rotor drag-lift ratios for test helicopter in autorotative flight. Theoretical curves computed for average $C_T = 0.0052$.
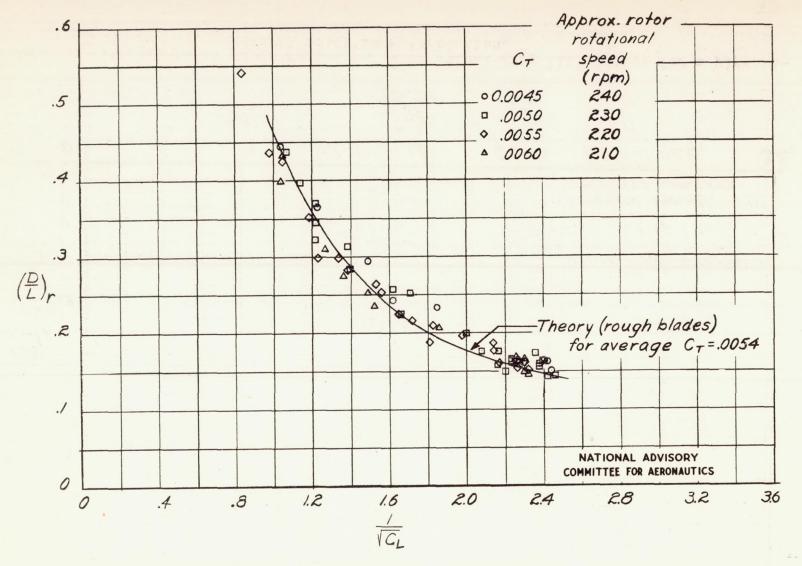
Fig. 8

Fig. 9

Figure 9.— Comparison of power-on experimental and theoretical main-rotor drag-lift ratios for test helicopter in the level-flight condition. (Experimental data from reference 1.)
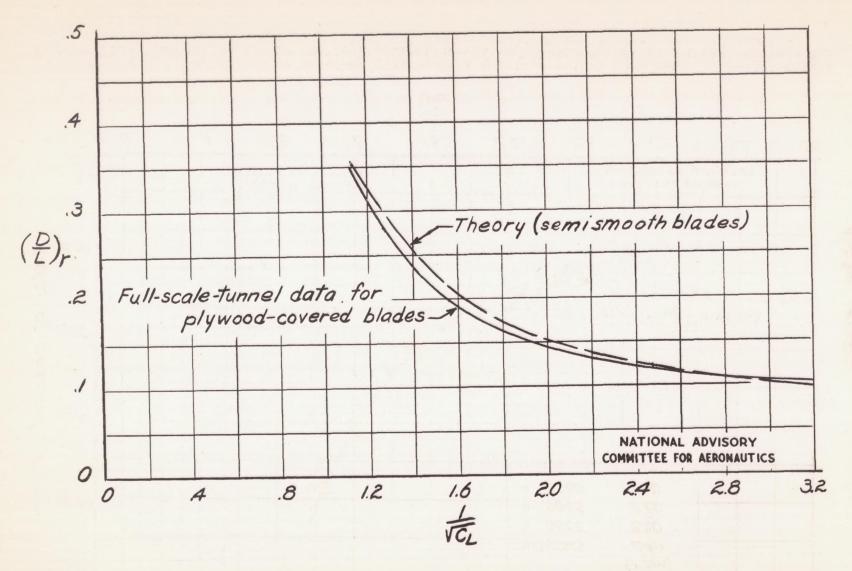
Figure 10.— Comparison of experimental and theoretical drag-lift ratios for a plywood-covered rotor in autorotation.
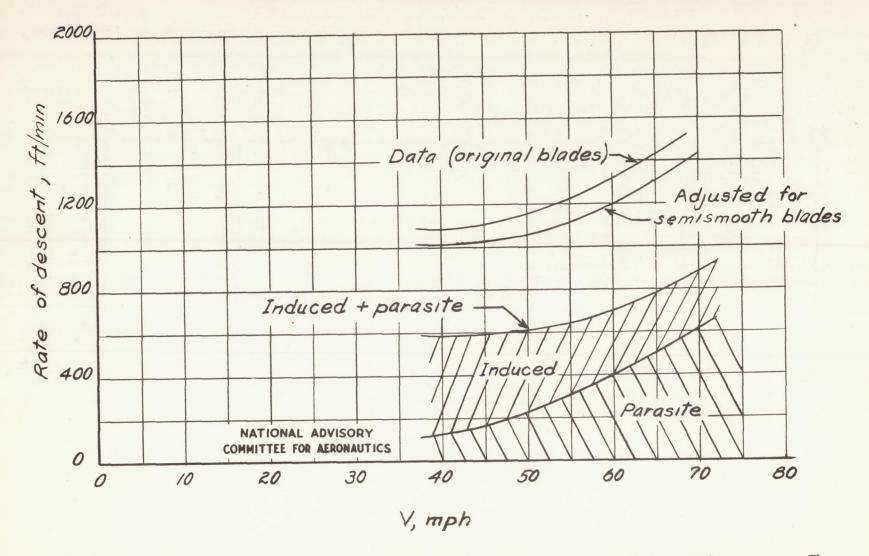
Fig. 10

Fig. 11

Figure 11.- Effect of main-rotor profile drag on autorotative glide performance. The increment between "original blade" and "semismooth" blade curves was calculated theoretically.